

Contextuality in infinite one-dimensional translation-invariant local Hamiltonians: strengths and limits

Kaiyan Yang,^{1,2} Xiao Zeng,^{1,3} Yujing Luo,¹ Guowu Yang,³ Lan Shu,² Miguel Navascués,⁴ and Zizhu Wang¹

¹*Institute of Fundamental and Frontier Sciences,
University of Electronic Science and Technology of China,
Chengdu 610054,
China*

²*School of Mathematical Sciences,
University of Electronic Science and Technology of China,
Chengdu 611731,
China*

³*School of Computer Science and Engineering,
University of Electronic Science and Technology of China,
Chengdu 611731,
China*

⁴*Institute for Quantum Optics and Quantum Information - IQOQI Vienna,
Austrian Academy of Sciences,
Boltzmannngasse 3, 1090 Vienna,
Austria*

In recent years there has been a growing interest in treating many-body systems as Bell scenarios, where lattice sites play the role of distant parties and only near-neighbor statistics are accessible. We investigate contextuality arising from three Bell scenarios in infinite, translation-invariant 1D models: nearest-neighbor with two dichotomic observables per site; nearest- and next-to-nearest neighbor with two dichotomic observables per site and nearest-neighbor with three dichotomic observables per site. For the first scenario, we give strong evidence that it cannot exhibit contextuality, not even in non-signaling physical theories beyond quantum mechanics. For the second one, we identify several low-dimensional models that reach the ultimate quantum limits, paving the way for self-testing ground states of quantum many-body systems. For the last scenario, which generalizes the Heisenberg model, we give strong evidence that, in order to exhibit contextuality, the dimension of the local quantum system must be at least 3.

INTRODUCTION

In a many-body quantum system, correlations appear as one of the most common manifestations of the quantum nature of the system. Different types of correlations, such as entanglement, EPR steering and nonlocality, were identified over the years and found applications in various quantum information processing tasks. Out of these types of correlations, nonlocality is the strongest and most difficult to test (Brunner *et al.*, 2014; Scarani, 2019). While experiments exploiting entanglement to teleport photons date back to the 90s (Bouwmeester *et al.*, 1997), nonlocality passed the most stringent experimental tests only in 2015 (Giustina *et al.*, 2015; Hensen *et al.*, 2015; Shalm *et al.*, 2015). One of the key assumptions in any nonlocality experiment is keeping the different parties space-like separated. In a many-body quantum system, however, this assumption may be too formidable to be overcome.

In recent years, the exploration of contextuality in quantum many-body systems has been a fruitful endeavor. Contextuality witnesses adapted from Bell inequalities have been tested in Bose-Einstein condensates (Schmied *et al.*, 2016; Tura *et al.*, 2014a). Translation and permutation symmetry allowed the full characterization of contextuality witnesses in many-body systems through bipartite correlators only (Tura *et al.*, 2015, 2017, 2014b; Wang *et al.*,

2017) (see (De Chiara and Sanpera, 2018) for a review). However, very little is known about the strengths and limits of the quantum models which violate these witnesses.

In this work, building on earlier characterizations of classical local behavior in many-body systems (Wang *et al.*, 2017), we investigate under which conditions the n -nearest neighbor statistics of a translation-invariant 1D quantum system evidence that the latter is contextual, by exploiting the connection between contextuality and Bell nonlocality. We focus on three different Bell scenarios, which differ on the number of measurement settings available to each party and the size of the near-neighbor marginals considered.

Our results show that some *a priori* promising Bell scenarios are unlikely to show any form of contextuality, even if we allow greater-than-quantum correlations. In other scenarios, we give evidence that some Bell inequalities require quantum systems of high enough local dimension to be violated. More interestingly, for several Bell inequalities, we find the maximum violation compatible with the laws of quantum mechanics, and identify the Hamiltonians achieving it. The ground states of contextual Hamiltonians are entangled, even though locally they may appear separable. As shown in (Wang *et al.*, 2017), it is possible to estimate the size at which the reduced density matrix of a quantum state becomes entangled, just by computing the difference between its average energy and the classical bound.

Since the former can be easily estimated in essentially any Noisy Intermediate-Scale Quantum (NISQ) device, one can think of our contextuality witnesses as robust entanglement benchmarks for future quantum simulators. From a more fundamental perspective, identifying the maximum quantum violation of a k -local Bell functional opens the possibility to falsify quantum theory in the many-body regime. Indeed, given access to a NISQ device, we can represent the local measurements and the state preparation of the corresponding Bell test through a vector of lab controls θ . By estimating the gradient of the Bell functional with respect to the variables θ , we can sequentially update the latter so as to minimize the observed value of the Bell functional in the device (effectively mimicking the working principle of the variational quantum eigensolver (Peruzzo *et al.*, 2014)). If it so happened that the final value of the Bell functional were below the quantum limit, then we would have disproven the universal validity of quantum theory, despite the lack of an alternative theoretical model.

One-dimensional quantum systems are the simplest many-body ensembles one can control in the lab. They can be found in natural condensed matter systems, as well as implemented via optical lattices or ion traps. For some such systems the only experimentally available data are near-neighbor correlators averaged over the whole chain (the so-called *structure factors*). As shown in (Wang *et al.*, 2017), in the regime of large system size, structure factors correspond to the near-neighbor correlators of an infinite, translation-invariant chain. Comprehending Bell nonlocality in large 1D systems hence requires us to characterize near-neighbor correlations in classical, quantum and supra-quantum translation-invariant systems.

The correlations $P(a_1, \dots, a_n | x_1, \dots, x_n)$ generated by n space-like separated classical systems with (classical) inputs $x_i, i \in 1, \dots, n$ and outputs $a_i, i \in 1, \dots, n$ admit a decomposition of the form:

$$P(a_1, \dots, a_n | x_1, \dots, x_n) = \int P(a_1 | x_1, \lambda) \dots P(a_n | x_n, \lambda) P(\lambda) d\lambda, \quad (1)$$

where λ is a set of hidden variables with probability distribution $P(\lambda)$. The distributions $P(\lambda)$ and $\{P(a_i | x_i, \lambda)\}_{i=1}^n$ are hence a *local hidden variable model* for the observed correlations $P(a_1, \dots, a_n | x_1, \dots, x_n)$. In Bell tests, different parties are required to be space-like separated, which can be seen as the physical realization of the independence of probabilities in (1). However, in a many-body quantum system, such a requirement is too formidable to overcome. As a result, when we assume that Eq. (1) holds in a quantum many-body system, what we are actually testing is contextuality (Budroni *et al.*, 2021; Kochen and Specker, 1967). The connection between contextuality and Bell nonlocality had been known since the 70s. Every Bell inequality can be regarded as a contextuality witness; the other direction is less systematic (Cabello, 2021). The role of contextuality,

especially of the Kochen-Specker type, in quantum computation has been actively investigated in recent years (for a review see (Budroni *et al.*, 2021)). It can be shown to be the source of the quantum advantage in several scenarios in quantum computation (Bermejo-Vega *et al.*, 2017; Bravyi *et al.*, 2018, 2020; Howard *et al.*, 2014). Most of these scenarios are constructed from the stabilizer formalism with magic states. While a hidden variable model for this formalism has been found recently (Zurel *et al.*, 2020), the model itself is contextual (Budroni *et al.*, 2021).

Our starting point is thus a Bell scenario with infinitely many parties in a chain, labeled by the integer numbers. At site $i \in \mathbb{Z}$, the corresponding party can conduct a measurement $x_i \in \{1, \dots, X\}$, obtaining the result $a_i \in A$. Since we assume translation invariance, the measurement statistics observed by any m consecutive parties equal those of parties, $1, \dots, m$, that is, $P_{1, \dots, m}(a_1, \dots, a_m | x_1, \dots, x_m)$. Any Bell scenario in the translation-invariant chain can therefore be fully specified by the three natural numbers $m, X, |A|$. Consequently, in this paper, a Bell scenario where only nearest-neighbor correlations are available and each party can conduct two dichotomic observables will be called the *222-scenario*. Extending the interaction distance to next-to-nearest neighbors gives us the *322-scenario*. Heisenberg-like Bell scenarios, with nearest-neighbor interactions but three dichotomic observables per site correspond to the *232-scenario*.

We say that an m -partite distribution $P_{1, \dots, m}(a_1, \dots, a_m | x_1, \dots, x_m)$ is no-signaling (Popescu and Rohrlich, 1994) if, for all $i \in \{1, \dots, m\}$,

$$\sum_{a_i} P_{1, \dots, m}(a_1, \dots, a_m | x_1, \dots, x_i, \dots, x_m) = \sum_{a_i} P_{1, \dots, m}(a_1, \dots, a_m | x_1, \dots, \tilde{x}_i, \dots, x_m), \quad (2)$$

for all pairs of measurement settings $x_i, \tilde{x}_i \in X$. Intuitively, this condition signifies that the statistics of the remaining $m-1$ parties are not affected by the choice of measurement setting of party i . Hence, party i cannot instantaneously transmit information to others.

Some no-signalling distributions $P_{1, \dots, m}(a_1, \dots, a_m | x_1, \dots, x_m)$ can be shown not to arise out of an infinite no-signalling TI system. This idea is formalized in the following definition: we say that $P_{1, \dots, m}(a_1, \dots, a_m | x_1, \dots, x_m)$ admits a TI no-signalling extension if there exists a mapping Q from finite sets $B \subset \mathbb{Z}$ to no-signalling $|B|$ -partite measurement statistics $Q_B(a_B | x_B)$ with the following properties:

1.

$$\sum_{a_{B \setminus C}} Q_B(a_{B \setminus C}, a_C | x_{B \setminus C}, x_C) = \sum_{a_{D \setminus C}} Q_D(a_{D \setminus C}, a_C | x_{D \setminus C}, x_C),$$

for all finite sets $B, C, D \subset \mathbb{Z}$, with $C \subset B, D$ (compatibility).

2. $Q_B = Q_{B+z}$, for all $z \in \mathbb{Z}$ (translation invariance).
3. $Q_{1,\dots,n} = P_{1,\dots,n}$ (consistency with observed statistics).

We call TI-NS the set of all distributions $P_{1,\dots,m}(a_1, \dots, a_m | x_1, \dots, x_m)$ admitting a no-signalling, translation-invariant extension.

The existence of a no-signalling extension is just a prerequisite for the existence of an overall infinite translation-invariant state. Whether such an entity exists at all depends also on the physics generating the observed correlations. We say that $P_{1,\dots,m}(a_1, \dots, a_m | x_1, \dots, x_m)$ admits a TI classical extension if it admits a NS extension Q and there exist distributions $P(\lambda), \{P_i(a|x, \lambda) : i \in \mathbb{Z}\}$ such that, for all N ,

$$Q_{-N,\dots,N}(a_{-N}, \dots, a_N | x_{-N}, \dots, x_N) = \sum_{\lambda} P(\lambda) \prod_{i=-N}^N P_i(a_i | x_i, \lambda). \quad (3)$$

We call TI-LHV the set of all distributions $P_{1,\dots,m}(a_1, \dots, a_m | x_1, \dots, x_m)$ admitting a TI classical extension.

Analogously, $P_{1,\dots,m}(a_1, \dots, a_m | x_1, \dots, x_m)$ admits a TI quantum extension if it admits a NS extension Q and there exist a Hilbert space \mathcal{H} , measurement operators $E_{a|x} : \mathcal{H} \rightarrow \mathcal{H}$, with $\sum_a E_{a|x} = \mathbb{I}$, and a translation-invariant quantum state ρ on the infinite chain with local Hilbert space \mathcal{H} such that, for all N ,

$$Q_{-N,\dots,N}(a_{-N}, \dots, a_N | x_{-N}, \dots, x_N) = \text{tr} \left\{ \bigotimes_{j=-N}^N E_{a_j | x_j} \rho_{-N,\dots,N} \right\}. \quad (4)$$

We call TI-Q the set of all distributions $P_{1,\dots,m}(a_1, \dots, a_m | x_1, \dots, x_m)$ admitting a TI quantum extension.

In (Wang *et al.*, 2017), two of us provided a full characterization of the set of m -nearest neighbor correlations admitting a TI classical extension. This set happens to be a polytope, i.e., a convex set defined by a finite number of linear inequalities or *facets*. When all local measurements are dichotomic ($|A| = 2$), one can regard any measurement x by party i as an observable σ_x^i with possible values ± 1 , and specify any no-signaling m -nearest neighbor distribution $P(a_1, \dots, a_m | x_1, \dots, x_m)$ through the averages of the different products of the observables $\sigma_{x_1}^1, \dots, \sigma_{x_m}^m$. For $m = 2$, in this ‘observable representation’ a facet would take the form

$$\sum_{x=1,\dots,X} J_x \langle \sigma_x^1 \rangle + \sum_{x,y=1,\dots,X} J_{xy} \langle \sigma_x^1 \sigma_y^2 \rangle \geq L_J. \quad (5)$$

Should the observed one-particle averages $\{\langle \sigma_x^1 \rangle : x \in X\}$ and nearest-neighbor two-point correlators $\{\langle \sigma_x^1 \sigma_y^2 \rangle :$

$x, y \in X\}$ of a TI system violate a facet of the classical (also called ‘local’) polytope, the corresponding many-body system would be shown not to admit a description compatible with classical physics.

The left hand side of Eq. (5) can be interpreted as a *Bell functional* that acts linearly on the distribution $P_{1,\dots,m}(a_1, \dots, a_m | x_1, \dots, x_m)$. Minimizing it over all distributions admitting a TI quantum extension, we obtain the *quantum limit* Q_J of the Bell functional J .

In the following, we describe a method that, for any $d \in \mathbb{N}$, carries such a minimization variationally over TI quantum systems of local dimension d , thus obtaining an upper bound Q_d on Q_J . The method also returns a concrete TI quantum system, with $\dim(H) = d$, achieving the Bell value Q_d with measurement operators $\{E_{a|x} : a, x\}$. Most statistical models studied in the literature use projective measurements, i.e. $\{E_{a|x} : a, x\}$ are projectors. For most of our results we only consider projective measurements, with one notable exception. When we need to verify that no 232-type Hamiltonian can violate the classical bound when $d = 2$, only considering projective measurements is too restrictive. Therefore for these Hamiltonians we allow fully general complex positive operator-valued measurements (POVMs) as their local observables, using a modified version of the algorithm presented in the following section to perform the optimization.

RESULTS

Upper bounding the ground state energy density

To minimize the left-hand side of expressions of the form (5), we start from the following observation: let $\{\sigma_x : \mathbb{C}^d \rightarrow \mathbb{C}^d : x \in X\}$ be a set of d -dimensional Hermitian operators with spectrum contained in $\{1, -1\}$. Then, the minimum value of (5) over all TI quantum states corresponds to the minimum energy-per site of the TI Hamiltonian

$$\mathcal{H}_{222}(\sigma_1, \dots, \sigma_m) = \sum_{i \in \mathbb{Z}} \sum_{x=1,\dots,X} J_x \sigma_x^i + \sum_{x,y=1,\dots,X} J_{xy} \sigma_x^i \sigma_y^{i+1}. \quad (6)$$

Tools from condensed matter physics such as uniform matrix product states (uMPS) (Vanderstraeten *et al.*, 2019) allow us to compute the desired energy density efficiently. In order to minimize (5) for a given local dimension d , all we have to do is suitably explore the manifold of the set of local observables, e.g.: via gradient descent.

Our first step consists of finding a parametrization of all the local observables. Consider observables $\{\sigma_a | a \in X\}$, each of which can be diagonalized by an unitary matrix U_a as

$$\sigma_a = U_a \Lambda_a U_a^\dagger, \quad (7)$$

where Λ_a is a diagonal matrix with entries ± 1 . To make this

more explicit, we use the vector $[n_x, n_y]$ to describe number of -1 in the eigenvalues σ_x and σ_y .

We can then use the space of skew-Hermitian matrices to effectively parameterize each U_a as

$$U_a = e^{S_a}, \quad (8)$$

where S_a is skew-Hermitian. Let $\{B_1, B_2, \dots, B_n\}$ be a basis of the vector space of skew-Hermitian matrices. Here $n = d^2 - d$ denotes the dimension of the space. Expanding S_a in this basis gives

$$S_a(W_a) = \sum_{k=1}^n w_{ak} B_k, \quad (9)$$

where $W_a \equiv \{w_{a1}, w_{a2}, \dots, w_{an}\}$ are scalars. Our optimization parameters are therefore $\{w_{ak} | a \in X; k = 1, \dots, n\}$.

Using the method above, observables $\sigma_a (a = x, y)$ in \mathcal{H}_{222} can be parameterized as

$$\sigma_a(W_a) = (e^{\sum_{k=1}^n w_{ak} B_k}) \Lambda_a (e^{\sum_{k=1}^n w_{ak} B_k})^\dagger. \quad (10)$$

Consequently, \mathcal{H}_{222} is parameterized as $\mathcal{H}_{222}(W_x, W_y)$.

Using Jordan's lemma (Scarani, 2019), the number of real parameters can be reduced when $|X| = 2$. For example, applying Jordan's lemma to \mathcal{H}_{222} when $d = 4$ yields a basis in which both σ_x and σ_y are block-diagonal:

$$\sigma_x = \begin{bmatrix} \sigma_{x,1} & \mathbf{0} \\ \mathbf{0} & \sigma_{x,2} \end{bmatrix}, \quad \sigma_y = \begin{bmatrix} \sigma_{y,1} & \mathbf{0} \\ \mathbf{0} & \sigma_{y,2} \end{bmatrix} \quad (11)$$

where $\sigma_{x,1}, \sigma_{x,2}, \sigma_{y,1}, \sigma_{y,2}$ are 2×2 Hermitian matrices.

We are now ready to present our MPS based gradient descent method. The method is iterative. For $a = x, y$, let $W_a(k)$ denote the parametrization of observable σ_a at the k -th iteration. We will refer to the parametrization $\{W_x(k), W_y(k)\}$ of both observables as $W(k)$. At each iteration k , the parameters $W(k)$ are updated to $W(k+1)$ through the following procedure.

First, we minimize the energy-per-site of the Hamiltonian $\mathcal{H}_{222}(k) \equiv \mathcal{H}_{222}(\sigma_a(k), \sigma_b(k))$ over the manifold of uMPS. The result $e(k)$ can be computed using, e.g., the Time-dependent Variational Principle (TDVP) algorithm (Haegeman et al., 2011; Milsted et al., 2013; Vanderstraeten et al., 2019) or the Variational Uniform Matrix Product State (VUMPS) algorithm (Vanderstraeten et al., 2019; Zauner-Stauber et al., 2018). We mainly use the TDVP algorithm for its good numerical stability and reasonable speed of convergence.

Following the TDVP algorithm, $e(k)$ can be expressed as

$$e(k) = \sum_{s,t,u,v} h(k)_{st}^{uv} \text{Tr}[A^t(k)^\dagger A^s(k)^\dagger l(k) A^u(k) A^v(k) r(k)], \quad (12)$$

where $\sum_{s,t,u,v} h(k)_{st}^{uv} |s\rangle \langle u| \otimes |t\rangle \langle v|$ is the local term of $\mathcal{H}_{222}(k)$; $\{A^s(k)\}_s \subset \mathbb{C}^{D \times D}$ is the tensor defining the optimal

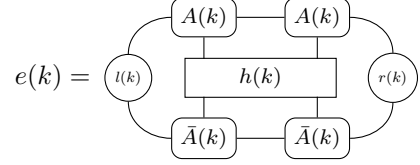


FIG. 1 Energy density

uMPS, and $l(k), r(k)$ are the left and right leading eigenvectors of the transfer matrix $T(k) = \sum_{s=1}^d \bar{A}^s(k) \otimes A^s(k)$.

Next, we seek to find observables leading to a Hamiltonian with a smaller energy-per-site, when evaluated over the uMPS with tensor $\{A^s(k)\}$ just identified. Hence, with $A(k)$ fixed, we replace the local term $h(k)$ by $h(\sigma_x(W), \sigma_y(W))$ in Eq.(12). This leads to a function $e(W; k)$ of the parameters W defining the observables. To update the parameters $W(k)$, we move away from $W(k)$ in the direction of maximum function decrease at point $W(k)$. That is, we move against the gradient of $e(W; k)$:

$$W(k+1) = W(k) - \gamma(k) \cdot \nabla_W e(W; k). \quad (13)$$

Here $\gamma(k)$ is a scaling parameter, which we take to be of the form $\gamma(k) = \max(\gamma_0 \alpha^{q(k)}, \gamma_{\min})$, where $\alpha \in (0, 1)$ and $q(k)$ is linear with respect to the iteration number k .

Starting from an initial seed $W(0)$, we iterate the two steps above, hence generating a sequence of parameter values $(W(0), W(1), \dots)$. At every iteration k , we check the condition $\|\nabla e(W; k)\|_2 < \epsilon^*$, for some desired convergence threshold ϵ^* . If the condition holds, we stop the algorithm and return the optimal parameters $W^* \equiv W(k)$.

In our experience, the quantity $e(W^*)$ is typically a very good estimate of the lowest quantum value of the considered contextuality functional over TI quantum systems of local dimension d . If e^* happens to be smaller than the classical bound of the corresponding facet inequality, then we can state that the found quantum system characterized by the TI Hamiltonian $\mathcal{H}_{222}(W^*)$ exhibits contextuality.

To test the algorithm, we apply it to compute the minimum ground state energy densities \mathcal{Q}_d ($d = 2, 3, 4$) of six 322-type TI quantum systems introduced in Sec. . All the results are plotted in Fig. 2. We find that the initial ground state energy densities determined by random parameters typically do not violate the classical bound \mathcal{L}_{322} (red line). As the iteration number increases, \mathcal{Q}_2 and \mathcal{Q}_3 decrease approximately linearly and begin to show contextuality. In Fig. 2(e) and Fig. 2(f), \mathcal{Q}_4 oscillates during the first several iterations. As the optimization process continues, \mathcal{Q}_4 also begins to cross \mathcal{L}_{322} after. The ground state energy densities of all six models converge to values below their classical bounds within 20 iterations.

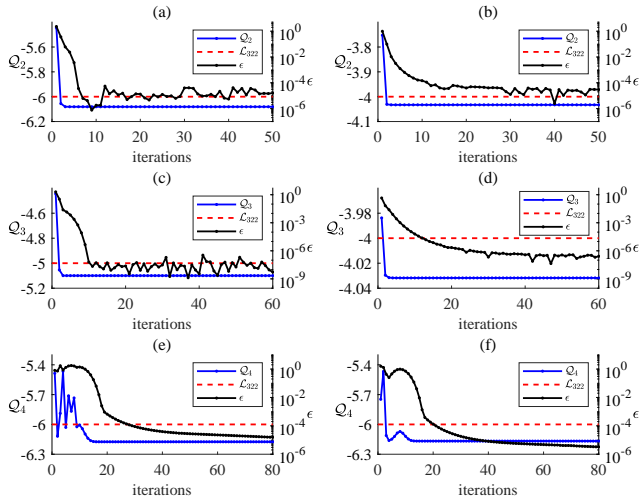


FIG. 2 Convergences of ground state energy density Q_d (blue line) and two-norm of gradient ϵ (black line) for 322-type TI quantum systems with the local observable dimension $d = 2, 3, 4$. The red dashed line represents the classical bound, and the regions below show contextuality. (a) Q_2 of No.1 in Table VI. (b) Q_2 of No.38 in Table VI. (c) Q_3 of No.7 in Table VI. (d) Q_3 of No.30 in Table VI. (e) Q_4 of No.37 in Table VI. (f) Q_4 of No.54 in Table VI.

Lower bounding the ground state energy density

Consider the scenario shown in Fig. 3: an infinite chain of elephants, each of which represents a physical system, be it quantum, classical or else. Call ϵ the overall state of the chain. Depending on the context, ϵ will be a classical probability distribution, a quantum state or a no-signaling box. Because ϵ is TI, the marginal distribution or the reduced state of each of the 5 marked elephants, taken from an arbitrary contiguous subset of the chain, should be equal: $\epsilon_1 = \dots = \epsilon_5$. Moreover, the reduced state of any contiguous subset of elephants should also be equal: $\epsilon_{1,\dots,1+k} = \epsilon_{2,\dots,2+k}, \forall 1 \leq k \leq 3$. When $k = 3$, the marginals/reduced states are shown in Fig. 3 as green and red rectangles. For any contiguous subset of ϵ of length l , the marginals/reduced states are said to be *locally translation-invariant* (LTI) if

$$\epsilon_{1,\dots,l-1} = \epsilon_{2,\dots,l}. \quad (14)$$

Clearly, LTI is a necessary condition for ϵ to be TI. For classical probability distributions in 1D, LTI is also sufficient: any LTI marginal can be extended to an infinite TI distribution (Goldstein *et al.*, 2017). In fact, this property is the key to the characterization of the set TI-LHV presented in (Wang *et al.*, 2017).

Unfortunately, LTI is not enough to characterize the near-neighbor density matrices of TI quantum states or even the near-neighbor marginals of TI no-signaling systems. In those scenarios LTI can be used to relax the set of such marginals, rather than to fully characterize it. Define thus LTI_n -NS as the set of boxes admitting an extension to an

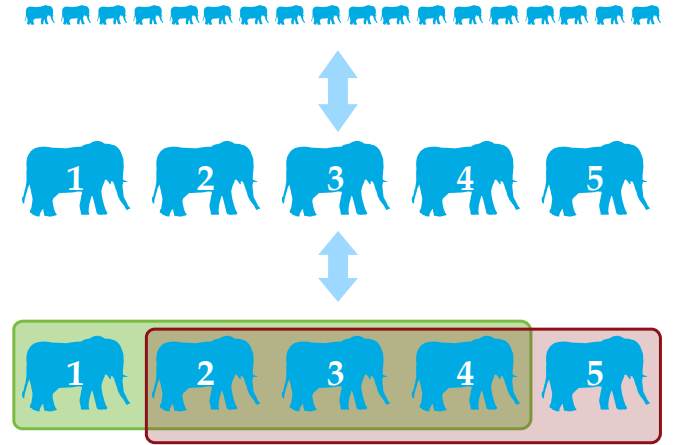


FIG. 3 Local translation invariance. A necessary condition from the requirement that the entire system is translation-invariant.

n -partite no-signaling box with local translation invariance. As shown in (Wang *et al.*, 2017), the distance between any element of the set LTI_n -NS and its subset TI-NS is upper bounded by $O(\frac{1}{n})$.

A straightforward extension to bound TI-Q is impossible, as the approximate characterization of general multipartite quantum correlations is an undecidable problem (Ji *et al.*, 2020). One can, however, relax the existence of quantum states and observables reproducing the observed correlations to that of positive semidefinite *moment matrices*. Those are matrices Γ whose rows and columns are labeled by monomials of measurement operators with at most s (the order of the relaxation) measurement operators per party, and where each entry $\Gamma_{\alpha\beta}$ is supposed to represent the quantity $\langle \alpha^\dagger \beta \rangle$, see (Navascués *et al.*, 2007; Navascués *et al.*, 2008) for details. In order to bound TI-Q, we demand the existence of a moment matrix for an n -partite Bell scenario and then impose LTI over the said moment matrix. Call LTI_n -NPA $_s$ the corresponding relaxation.

For any Bell functional, we can thus find a lower bound on its minimal value in TI-NS and TI-Q by respectively optimizing over LTI_n -NS (with linear programming techniques (Matoušek and Gärtner, 2007)) and LTI_n -NPA $_s$ (with semidefinite programming techniques (Gärtner and Matoušek, 2012)). Moreover, one can improve those lower bounds by increasing the values of n, s .

Contextuality in 222-type Hamiltonians

The LTI-LHV polytope for 2 dichotomic observables has 36 facets. Computing their LTI_4 -NS lower bounds reveals that most of them coincide with the corresponding classical bounds. In fact, there is only one inequality, up to local relabeling, which can potentially show contextuality. In its

1D TI quantum Hamiltonian form, it reads

$$\mathcal{H}_{222} = \sum_{i=1}^{\infty} (2\sigma_x^i + \sigma_x^i \sigma_x^{i+1} + \sigma_x^i \sigma_y^{i+1} - \sigma_y^i \sigma_x^{i+1} - \sigma_y^i \sigma_y^{i+1}), \quad (15)$$

with classical bound -2 .

Lower bounding Eq. (15) with LTI_n -NS with increasing n , we observed some curious phenomena. Because exact optimal solutions of linear programs are rational numbers, we obtain the solutions in Table I.

n	3	4	5	6	7	8	9
LTI_n -NS lower bound	$-\frac{8}{3}$	$-\frac{12}{5}$	$-\frac{9}{4}$	$-\frac{13}{6}$	$-\frac{36}{17}$	$-\frac{48}{23}$	$-\frac{62}{30}$

TABLE I Exact solutions of LTI_n -NS approximations of the lower bound of (15) as a function of n .

The numerators and denominators in the table form two integer sequences: A027691 (The OEIS Foundation Inc., 2021a) and A152948 (The OEIS Foundation Inc., 2021b) in *The On-Line Encyclopedia of Integer Sequences*. Moreover, the displaced inverse of a quadratic function

$$-2 - \frac{4}{n^2 - 3n + 6}, \quad n \in \mathbb{N}, n \geq 3 \quad (16)$$

perfectly fits the sequence of lower bounds in Table I, see Fig. 4.

In the limit $n \rightarrow \infty$, this function converges to the classical bound -2 . In other words, if the solution of the optimization over LTI_n -NS satisfies (16) for all $n \geq 3$, then no Hamiltonian of the form (15), quantum or otherwise, can possibly violate the classical bound.

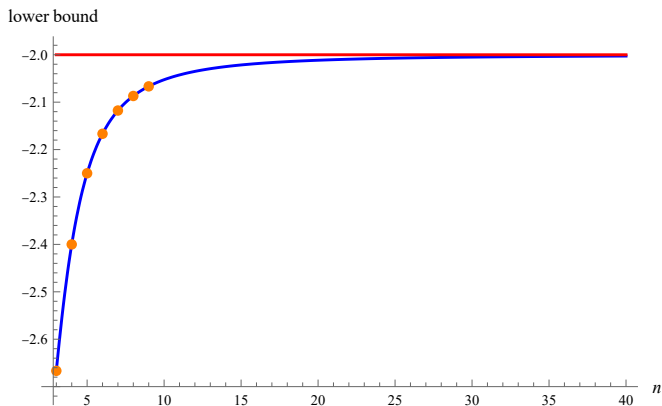


FIG. 4 Exact solutions for the LTI_n -NS approximation of the lower bound of Eq. 15 (orange dots), the fitted function (16) (blue line) when $3 \leq n \leq 40$, and the classical bound (red line).

Proving that a series of rational numbers, the solutions of linear programs of exponentially increasing size, converges to a certain value is very hard. However, we do have additional numerical evidence to support our claim that the

lowest possible ground state energy density of 1D TI quantum Hamiltonians of the form (15) is -2 . We used our algorithm, described in Section , to search for the quantum Hamiltonian with the lowest ground state energy density, for local observables of dimension $2 \leq d \leq 6$. For each d , σ_x and σ_y are parameterized by the method described below, and we find the lowest quantum value \mathcal{Q}_d among all possible systems is -2 . Moreover, the corresponding two-body reduced density matrix of the quantum system for the ground state is a rank 1 projector, which shows that the ground state is in fact a product state. We present these ground states and the parameters for observables in Table II.

TABLE II Ground state and parameters of \mathcal{H}_{222} under the different observable dimension settings when the ground state energy density equals to the classical bound -2 .

d	w_1	w_2	w_3	$[n_x, n_y]$	Ground state
2	0.00001	-	-	[1, 1]	$ 1\rangle^{\otimes \infty}$
3	0.65129	-	-	[2, 2]	$ 2\rangle^{\otimes \infty}$
4	0.00004	0.59946	-	[2, 2]	$ 3\rangle^{\otimes \infty}$
5	0.98662	0.00001	-	[2, 2]	$ 4\rangle^{\otimes \infty}$
6	0.90451	0.91913	0.00005	[3, 3]	$ 5\rangle^{\otimes \infty}$

To make sense of Table II, we next explicitly write the parametrization of the d -dimensional observables achieving the classical bound. Two 2×2 matrices having eigenvalues one and one -1 will repeatedly appear below: Λ is the diagonal matrix with diagonal entries ± 1 , $B(w)$ is a matrix governed by one parameter $\{w\}$:

$$\Lambda = \begin{bmatrix} 1 & 0 \\ 0 & -1 \end{bmatrix}, \quad B(w) = \begin{bmatrix} \cos(2w) & -\sin(2w) \\ -\sin(2w) & -\cos(2w) \end{bmatrix}. \quad (17)$$

When $d = 2$ is assigned to local observables in \mathcal{H}_{222} , σ_x is a diagonal matrix with diagonal entries 1 and -1 , i.e., $\sigma_x = \Lambda$, and σ_y determined by one parameter $\{w_1\}$ has the same parameterized form as $B(w)$, i.e., $\sigma_y(w_1) = B(w_1)$. In this case, $[n_x, n_y] = [1, 1]$ and σ_x, σ_y are of the form

$$\sigma_x = \Lambda, \quad \sigma_y(w_1) = B(w_1). \quad (18)$$

When $d = 3$ is assigned to local observables in \mathcal{H}_{222} , σ_x is a diagonal matrix with diagonal entries $(1, -1, -1)$. σ_y is a block diagonal matrix, where the main-diagonal blocks are one matrix $B(w_1)$ and one numerical value -1 . Then, $[n_x, n_y] = [2, 2]$ and σ_x, σ_y are given by

$$\sigma_x = \begin{bmatrix} \Lambda & \mathbf{0} \\ \mathbf{0} & -1 \end{bmatrix}, \quad \sigma_y(w_1) = \begin{bmatrix} B(w_1) & \mathbf{0} \\ \mathbf{0} & -1 \end{bmatrix}. \quad (19)$$

When $d = 4$ is assigned to local observables in \mathcal{H}_{222} , σ_x is a diagonal matrix with diagonal entries two 1 and two -1 , and σ_y is a block diagonal matrix with main-diagonal

blocks being two 2×2 matrices $B(w_1)$ and $B(w_2)$. In this case, $[n_x, n_y] = [2, 2]$ and σ_x, σ_y are of the forms

$$\sigma_x = \begin{bmatrix} \Lambda & \mathbf{0} \\ \mathbf{0} & \Lambda \end{bmatrix}, \quad \sigma_y(w_1, w_2) = \begin{bmatrix} B(w_1) & \mathbf{0} \\ \mathbf{0} & B(w_2) \end{bmatrix}. \quad (20)$$

When $d = 5$ is assigned to local observables in \mathcal{H}_{222} , σ_x is a diagonal matrix with diagonal entries two -1 and three 1 . σ_y is a block diagonal matrix, where the main-diagonal blocks are two 2×2 matrices $B(w_1)$ and $B(w_2)$ and one numerical number 1 . Then, $[n_x, n_y] = [2, 2]$ and σ_x, σ_y are given by

$$\sigma_x = \begin{bmatrix} \Lambda & & & \\ & \Lambda & & \\ & & \mathbf{0} & \\ & & & 1 \end{bmatrix}, \quad \sigma_y(w_1, w_2) = \begin{bmatrix} B(w_1) & & & \\ & B(w_2) & & \\ & & & \mathbf{0} \\ & & & & 1 \end{bmatrix}. \quad (21)$$

When $d = 6$ is assigned to local observables in \mathcal{H}_{222} , σ_x is a diagonal matrix, where three -1 and three 1 are alternately arranged in the diagonal. σ_y is a block diagonal matrix with main-diagonal blocks being three 2×2 matrices $B(w_1)$, $B(w_2)$ and $B(w_3)$. Then, $[n_x, n_y] = [3, 3]$ and σ_x, σ_y have the forms

$$\sigma_x = \begin{bmatrix} \Lambda & & & \\ & \Lambda & & \\ & & \mathbf{0} & \\ & & & \Lambda \end{bmatrix}, \quad (22)$$

$$\sigma_y(w_1, w_2, w_3) = \begin{bmatrix} B(w_1) & & & \\ & B(w_2) & & \\ & & & \mathbf{0} \\ & & & & B(w_3) \end{bmatrix}.$$

Contextuality in 322-type Hamiltonians

The TI-LHV polytope for the 322-type Hamiltonians has been characterized in (Wang *et al.*, 2017): it has 32372 facets which can be sorted into 2102 equivalence classes. The general form of the 322-type Hamiltonian is given by

$$\begin{aligned} \mathcal{H}_{322} = & \sum_{i=1}^{\infty} J_x \sigma_x^i + J_y \sigma_y^i + J_{xx}^{AB} \sigma_x^i \sigma_x^{i+1} + J_{xy}^{AB} \sigma_x^i \sigma_y^{i+1} \\ & + J_{yx}^{AB} \sigma_y^i \sigma_x^{i+1} + J_{yy}^{AB} \sigma_y^i \sigma_y^{i+1} + J_{xx}^{AC} \sigma_x^i \sigma_x^{i+2} \\ & + J_{xy}^{AC} \sigma_x^i \sigma_y^{i+2} + J_{yx}^{AC} \sigma_y^i \sigma_x^{i+2} + J_{yy}^{AC} \sigma_y^i \sigma_y^{i+2}, \end{aligned} \quad (23)$$

where $\{J_x, J_y, J_{xx}^{AB}, J_{xy}^{AB}, J_{yx}^{AB}, J_{yy}^{AB}, J_{xx}^{AC}, J_{xy}^{AC}, J_{yx}^{AC}, J_{yy}^{AC}\}$ are the couplings given by the facet inequalities and σ_x, σ_y are local observables.

Using our uMPS based gradient descent algorithm, a total of 63 Hamiltonians exhibit contextuality. The explicit parameterization of observables σ_x and σ_y is explained at the end of this section. All the contextual Hamiltonians and ground state energy densities are listed in Table V and Table VI respectively. Among them, we identify some quantum models whose ground state energy density matches the

LT_I₅-NPA₁ lower bounds. For all these contextuality witnessess, we have thus identified translation-invariant quantum models exhibiting the strongest quantum violation. All the matched models are summarized in Table III. As the reader can appreciate, the first five inequalities seem to require local dimension $d = 3$ to be saturated; inequality 6, dimension 4; and the last four inequalities, dimension 5.

TABLE III The ground state energy density \mathcal{Q}_d of ten 322-type TI quantum systems matches the LT_I₅-NPA₁ lower bound. The second column gives the number of each model in this table in Table VI.

No.	Table VI	\mathcal{L}	\mathcal{Q}_2	\mathcal{Q}_3	\mathcal{Q}_4	\mathcal{Q}_5	LT _I ₅ -NPA ₁
1	No.1	-6	-6.08108	-6.32747			-6.32747
2	No.2	-6	-6.10943	-6.33712			-6.33712
3	No.3	-3	-3.04150	-3.20711			-3.20711
4	No.4	-4	-	-4.14623			-4.14623
5	No.5	-8	-	-8.12123			-8.12123
6	No.6	-4	-	-4.02415	-4.10310		-4.10310
7	No.7	-5	-	-5.09951	-5.09951	-5.29852	-5.29852
8	No.8	-4	-	-4.18655	-4.18655	-4.33137	-4.33137
9	No.9	-4	-	-4.11581	-4.11581	-4.41421	-4.41421
10	No.10	-5	-	-5.07058	-5.07058	-5.26969	-5.26969

In Fig. 5, the reader can see the trajectories in parameter space followed by two quantum systems, of dimensions $d = 3$ and $d = 4$, undergoing our gradient descent method. This is possible because the number of free continuous parameters in one and another case are 1 and 2.

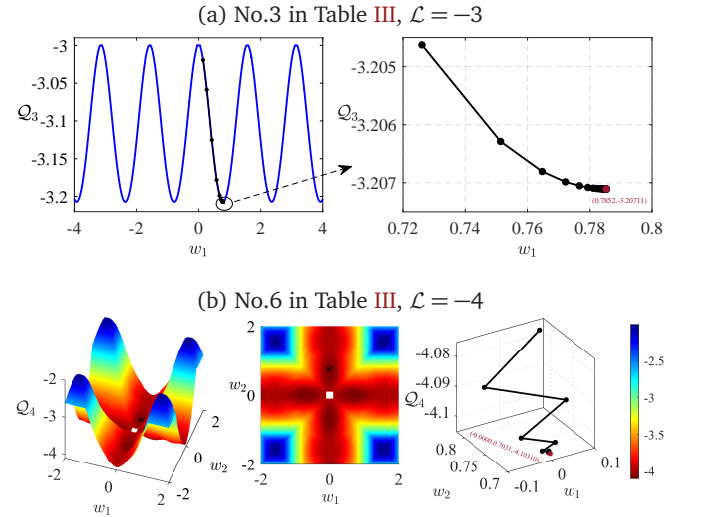


FIG. 5 The trajectory of the ground state energy density (black dotted line) of two models in Table III. (a) has two subplots, and the right one is an enlarged view for the trajectory in the left one when ground state energy density converges to the minimum. (b) has three subplots, the middle one is the top view of the leftmost one, and the rightmost one only depicts the trajectory.

In Fig. 5(a), \mathcal{Q}_3 surfaces (blue lines) show that the Hamiltonian exhibits contextuality no matter which values the parameter takes. The trajectory of ground state energy density (black dotted line) in the left subplot decreases along the \mathcal{Q}_3

surface to the bottom. Besides, the right enlarged subplot of the trajectory demonstrates that ground state energy density eventually converges to the respective LTI_n -NPA_s lower bound. In Fig. 5(b), the leftmost subplot shows the trajectory of the ground state energy density on the 3D \mathcal{Q}_4 surface, the middle 2D-subplot is the top view of the leftmost one, and the rightmost one only depicts the trajectory of the ground state energy density. Iteratively, our methods guide the initial random ground state energy density converging to the lowest possible one.

We plot the ground state energy density as functions of the parameters defining the local observables for some of the Hamiltonians in Table III and Table VI to gauge the robustness of the contextuality violations. Five models for $d = 4$ and another five models for $d = 5$ are shown in Fig. 6 and Fig. 7 respectively. Note that the first two models in Fig. 6(a)-(b) and the first four models in Fig. 7(a)-(d) exhibit the strongest contextuality.

It can be seen that some Hamiltonians are much more susceptible to small changes in parameters that define the local observables than others. For the Hamiltonians in Fig. 6(b), Fig. 7(b) and Fig. 7(c), keeping the ground state energy density above the classical bound is unstable, small perturbations in the parameters will make them violate it. In contrast, the remaining Hamiltonians need carefully engineered parameters to violate the classical bound. Especially for the Hamiltonian in Fig. 7(e), square-like parameter regions exist in which the corresponding ground state energy density could not violate the classical bound no matter how many times the perturbations are given. These plots help us find suitable Hamiltonians for simulation in trapped-ion or optical lattice systems, where witnessing contextuality (or the strongest contextuality) simply involves cooling the corresponding Hamiltonian to the ground state.

We next describe the parameterization of the 322-type Hamiltonians achieving the minimum quantum values in Table III. For $d = 2$ and $d = 4$, σ_x , σ_y have the exact same parameterized forms as the observables in the 222-type Hamiltonians in Eq. (18) and Eq. (20) respectively.

For $d = 3$ and $d = 5$, depending on the number of 1's and -1 's of each matrix Λ_a ($a = x, y$) in (7), two different classes of pairs of local observables σ_x and σ_y are considered. Here, we continue using the notations Λ and $B(w)$ introduced in (17).

For local dimension $d = 3$, the first class of pairs of local observables is of the form $[n_x, n_y] = [1, 2]$. More specifically:

$$\sigma_x = \begin{bmatrix} \Lambda & \mathbf{0} \\ \mathbf{0} & 1 \end{bmatrix}, \quad \sigma_y(w_1) = \begin{bmatrix} B(w_1) & \mathbf{0} \\ \mathbf{0} & -1 \end{bmatrix}. \quad (24)$$

The second class is of the form $[n_x, n_y] = [1, 1]$, with

$$\sigma_x = \begin{bmatrix} 1 & \mathbf{0} \\ \mathbf{0} & \Lambda \end{bmatrix}, \quad \sigma_y(w_1) = \begin{bmatrix} 1 & \mathbf{0} \\ \mathbf{0} & B(w_1) \end{bmatrix}. \quad (25)$$

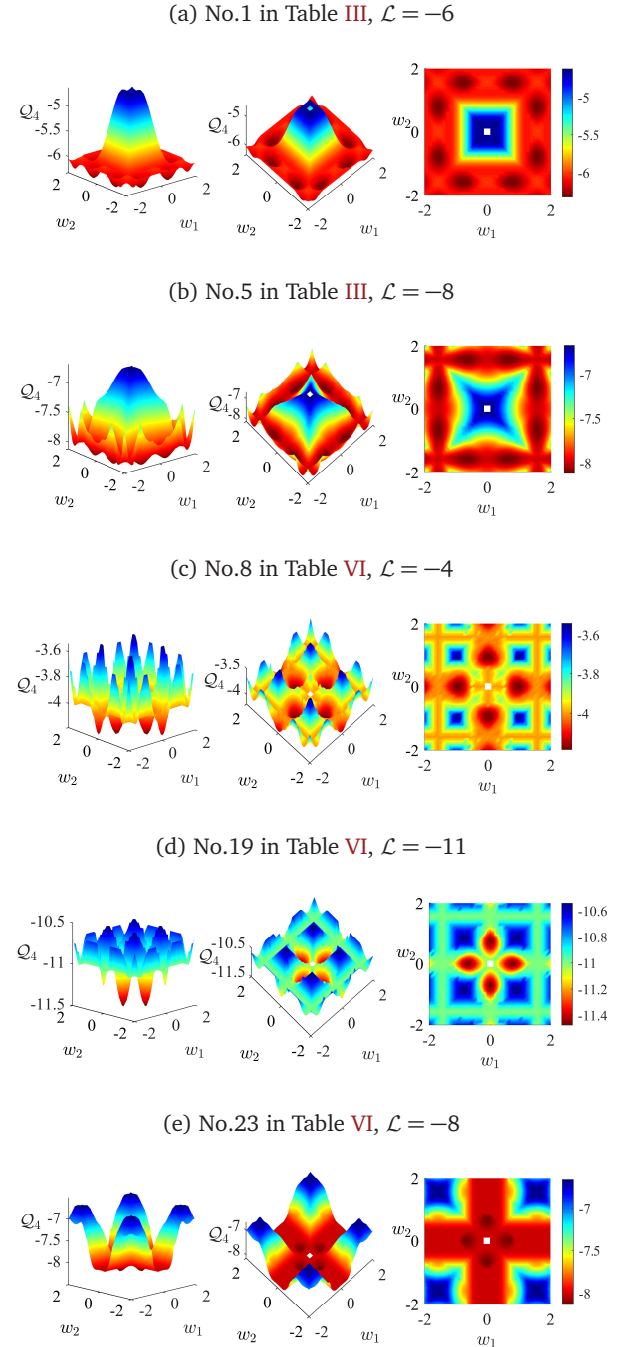


FIG. 6 \mathcal{Q}_4 surface of five models in Table III and Table VI, where w_1, w_2 both take discrete values on $[-2, 2]$ at the interval 0.1. Each model has three subplots. The leftmost is a 3D-surface, the middle figure is from another perspective of the left side one to view the internal structure, and the third one is the top view of the leftmost image.

For local dimension $d = 5$, the first class of observable

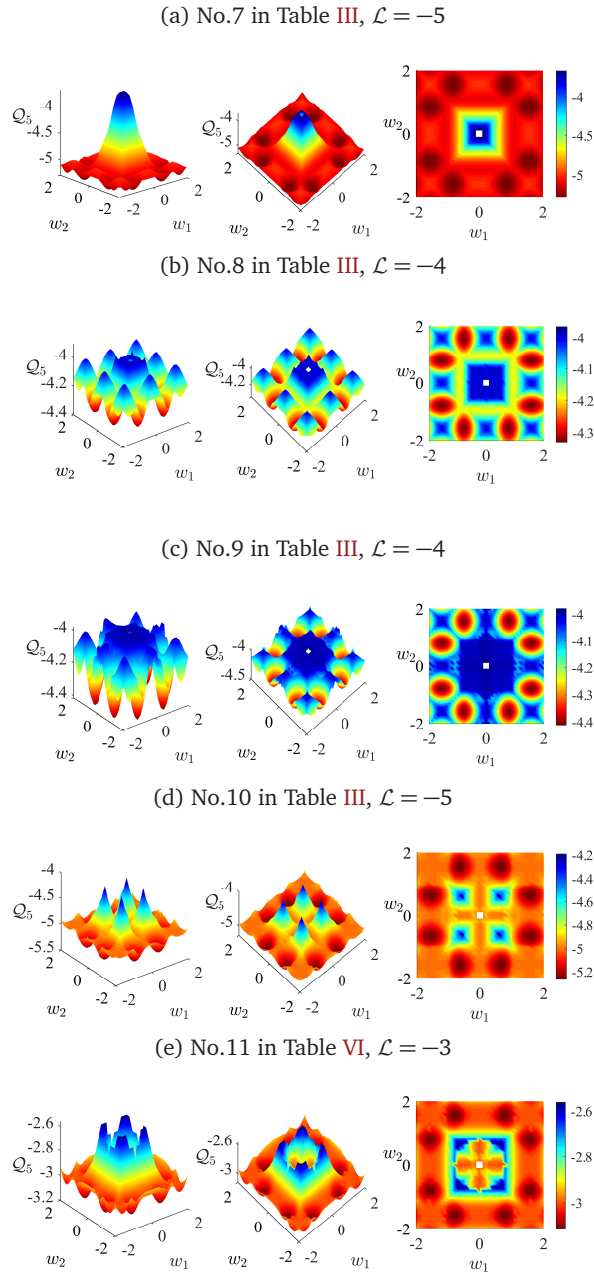


FIG. 7 Q_5 surface of five models in Table III and Table VI, where w_1, w_2 both take discrete values on $[-2, 2]$ at the interval 0.1. Each model has three subplots. The leftmost is a 3D-surface, the middle figure is from another perspective of the left side one to view the internal structure, and the third one is the top view of the leftmost image.

pairs is of the form $[n_x, n_y] = [2, 2]$, with

$$\sigma_x = \begin{bmatrix} \Lambda & & \mathbf{0} \\ & \Lambda & \\ \mathbf{0} & & 1 \end{bmatrix}, \quad \sigma_y(w_1, w_2) = \begin{bmatrix} B(w_1) & & \mathbf{0} \\ & B(w_2) & \\ \mathbf{0} & & 1 \end{bmatrix}. \quad (26)$$

The second class of observable pairs satisfies $[n_x, n_y] =$

$[3, 3]$, and σ_x and σ_y are given by

$$\sigma_x = \begin{bmatrix} \Lambda & & \mathbf{0} \\ & \Lambda & \\ \mathbf{0} & & -1 \end{bmatrix}, \quad \sigma_y(w_1, w_2) = \begin{bmatrix} B(w_1) & & \mathbf{0} \\ & B(w_2) & \\ \mathbf{0} & & -1 \end{bmatrix}. \quad (27)$$

Contextuality in 232-type Hamiltonians

The LTI-LHV polytope for 3 dichotomic observables has 92694 facets, which can be classified into 652 equivalent classes (Rosset, 2015). The general form of this type of Hamiltonian is given by

$$\begin{aligned} \mathcal{H}_{232} = & \sum_{i=1}^{\infty} J_x \sigma_x^i + J_y \sigma_y^i + J_z \sigma_z^i + J_{xx} \sigma_x^i \sigma_x^{i+1} + J_{xy} \sigma_x^i \sigma_y^{i+1} \\ & + J_{xz} \sigma_x^i \sigma_z^{i+1} + J_{yx} \sigma_y^i \sigma_x^{i+1} + J_{yy} \sigma_y^i \sigma_y^{i+1} + J_{yz} \sigma_y^i \sigma_z^{i+1} \\ & + J_{zx} \sigma_z^i \sigma_x^{i+1} + J_{zy} \sigma_z^i \sigma_y^{i+1} + J_{zz} \sigma_z^i \sigma_z^{i+1}. \end{aligned} \quad (28)$$

We consider \mathcal{H}_{232} when $d = 2, 3, 4$ and perform the optimizations on one representative facet from each of the 652 classes. For $d = 3, 4$, we only consider real parameters. For $d = 2$, we allow the most general measurements in quantum theory: complex POVMs. In the Method section, we present a projected gradient descent algorithm to optimize over the set of complex POVMs. All 652 Hamiltonians can only reach the classical bound up to numerical precision of 10^{-5} when $d = 2$, while for $d \geq 3$ there are many Hamiltonians which can violate the classical bound. The ground state energy densities of some contextual Hamiltonians are shown in Table IV, see Table VII for the couplings defining the contextuality witnesses. In addition, the parameters specifying the optimal local observables are listed in Table VIII for $d = 3$ and in Table IX for $d = 4$.

TABLE IV Ground state energy density for 5 232-type TI Hamiltonians under the dimension of local observables $d = 2, 3, 4$.

No.	\mathcal{L}	Q_2	Q_3	Q_4	LTI ₄ -NPA ₁
1	-9	-9.00000	-9.01875	-9.01875	-9.27833
2	-4	-4.00000	-4.03928	-4.03928	-4.20626
3	-5	-5.00000	-5.04162	-5.04162	-5.14754
4	-4	-4.00000	-4.01336	-4.11562	-4.23786
5	-2	-2.00000	-2.08094	-2.08749	-2.28767

The local observables σ_x, σ_y and σ_z are parametrized using the method presented in Section : for given Λ_a, S_a the local observable σ_a can be written as

$$\sigma_a = e^{S_a} \Lambda_a (e^{S_a})^\dagger. \quad (29)$$

While this step is straightforward, different combinations of ± 1 in Λ_a may lead to different ground state energy density.

Since the number of 1 and -1 on the diagonal of Λ_a in three local observables is not necessarily the same, there

is more than one combination of three parameterized local observables. We consider every possible combination of 1 and -1 in Λ_a for each $a \in \{x, y, z\}$. We only show combinations of parameterized local observables used in Table IV below. Here, we denote the 2×2 identity matrix by I , and continue using the notation Λ introduced in (17).

When $d = 2$, the classical bound can be achieved via three local observables determined by two parameters, where $[n_x, n_y, n_z] = [2, 1, 1]$. The first local observable σ_x is minus the identity matrix:

$$\sigma_x = \begin{bmatrix} -1 & 0 \\ 0 & -1 \end{bmatrix}. \quad (30)$$

For the second and third local observables $\sigma_a (a = y, z)$, Λ_a has entries one 1 and one -1 on the main diagonal, and S_a is determined by one parameter $\{w\}$. Hence, σ_y and σ_z are specified by

$$\begin{aligned} \Lambda_y &= \begin{bmatrix} 1 & 0 \\ 0 & -1 \end{bmatrix}, & S_y(w_1) &= \begin{bmatrix} 0 & w_1 \\ -w_1 & 0 \end{bmatrix}; \\ \Lambda_z &= \begin{bmatrix} 1 & 0 \\ 0 & -1 \end{bmatrix}, & S_z(w_2) &= \begin{bmatrix} 0 & w_2 \\ -w_2 & 0 \end{bmatrix}. \end{aligned} \quad (31)$$

For $d = 3$, two different combinations of three parameterized local observables are used, where the difference arises from Λ_a , but S_a of each local observable share the same parameterized form as

$$\begin{aligned} S_x(w_1, w_2, w_3) &= \begin{bmatrix} 0 & w_1 & w_2 \\ -w_1 & 0 & w_3 \\ -w_2 & -w_3 & 0 \end{bmatrix}, \\ S_y(w_4, w_5, w_6) &= \begin{bmatrix} 0 & w_4 & w_5 \\ -w_4 & 0 & w_6 \\ -w_5 & -w_6 & 0 \end{bmatrix}, \\ S_z(w_7, w_8, w_9) &= \begin{bmatrix} 0 & w_7 & w_8 \\ -w_7 & 0 & w_9 \\ -w_8 & -w_9 & 0 \end{bmatrix}. \end{aligned} \quad (32)$$

In the first combination, $[n_x, n_y, n_z] = [2, 1, 1]$, where Λ_x has one 1 and two -1 on the main diagonal, and Λ_y and Λ_z both have two 1 and one -1 being main diagonal entries. Then, Λ_x , Λ_y , and Λ_z are given by

$$\Lambda_x = \begin{bmatrix} \Lambda & \mathbf{0} \\ \mathbf{0} & -I \end{bmatrix}, \quad \Lambda_y = \begin{bmatrix} 1 & \mathbf{0} \\ \mathbf{0} & \Lambda \end{bmatrix}, \quad \Lambda_z = \begin{bmatrix} 1 & \mathbf{0} \\ \mathbf{0} & \Lambda \end{bmatrix}. \quad (33)$$

In the second combination, $[n_x, n_y, n_z] = [2, 1, 2]$, where Λ_x and Λ_z both have one 1 and two -1 on the main diagonal, and Λ_y has two 1 and one -1 being main diagonal entries. Then, Λ_x , Λ_y , and Λ_z are given by

$$\Lambda_x = \begin{bmatrix} \Lambda & \mathbf{0} \\ \mathbf{0} & -I \end{bmatrix}, \quad \Lambda_y = \begin{bmatrix} 1 & \mathbf{0} \\ \mathbf{0} & \Lambda \end{bmatrix}, \quad \Lambda_z = \begin{bmatrix} \Lambda & \mathbf{0} \\ \mathbf{0} & -I \end{bmatrix}. \quad (34)$$

For $d = 4$, four different classes of triples of local observables are used. These classes differ from each other on the

structure of the matrices Λ_a in (29). The matrices S_a have, nonetheless, the same form in the three classes, namely:

$$\begin{aligned} S_x(w_1, w_2, w_3, w_4, w_5, w_6) &= \begin{bmatrix} 0 & w_1 & w_2 & w_3 \\ -w_1 & 0 & w_4 & w_5 \\ -w_2 & -w_4 & 0 & w_6 \\ -w_3 & -w_5 & -w_6 & 0 \end{bmatrix}, \\ S_y(w_7, w_8, w_9, w_{10}, w_{11}, w_{12}) &= \begin{bmatrix} 0 & w_7 & w_8 & w_9 \\ -w_7 & 0 & w_{10} & w_{11} \\ -w_8 & -w_{10} & 0 & w_{12} \\ -w_9 & -w_{11} & -w_{12} & 0 \end{bmatrix}, \\ S_z(w_{13}, w_{14}, w_{15}, w_{16}, w_{17}, w_{18}) &= \begin{bmatrix} 0 & w_{13} & w_{14} & w_{15} \\ -w_{13} & 0 & w_{16} & w_{17} \\ -w_{14} & -w_{16} & 0 & w_{18} \\ -w_{15} & -w_{17} & -w_{18} & 0 \end{bmatrix}. \end{aligned} \quad (35)$$

The first class is of the form $[n_x, n_y, n_z] = [3, 1, 1]$, where Λ_x has one 1 and three -1 on the main diagonal, and Λ_y and Λ_z both have three 1 and one -1 being main diagonal entries. Then, Λ_x , Λ_y , and Λ_z are given by

$$\Lambda_x = \begin{bmatrix} \Lambda & \mathbf{0} \\ \mathbf{0} & -I \end{bmatrix}, \quad \Lambda_y = \begin{bmatrix} I & \mathbf{0} \\ \mathbf{0} & \Lambda \end{bmatrix}, \quad \Lambda_z = \begin{bmatrix} I & \mathbf{0} \\ \mathbf{0} & \Lambda \end{bmatrix}. \quad (36)$$

The second class is of the form $[n_x, n_y, n_z] = [3, 2, 3]$, where Λ_x and Λ_z both have one 1 and three -1 on the main diagonal, and Λ_y has two 1 and two -1 being main diagonal entries. Then, Λ_x , Λ_y , and Λ_z are given by

$$\Lambda_x = \begin{bmatrix} \Lambda & \mathbf{0} \\ \mathbf{0} & -I \end{bmatrix}, \quad \Lambda_y = \begin{bmatrix} \Lambda & \mathbf{0} \\ \mathbf{0} & \Lambda \end{bmatrix}, \quad \Lambda_z = \begin{bmatrix} \Lambda & \mathbf{0} \\ \mathbf{0} & -I \end{bmatrix}. \quad (37)$$

The third class is of the form $[n_x, n_y, n_z] = [3, 2, 1]$, where Λ_x has one 1 and three -1 on the main diagonal, Λ_y has two 1 and two -1 being main diagonal entries, and Λ_z takes three 1 and one -1 on the main diagonal. Then, Λ_x , Λ_y , and Λ_z are given by

$$\Lambda_x = \begin{bmatrix} \Lambda & \mathbf{0} \\ \mathbf{0} & -I \end{bmatrix}, \quad \Lambda_y = \begin{bmatrix} \Lambda & \mathbf{0} \\ \mathbf{0} & \Lambda \end{bmatrix}, \quad \Lambda_z = \begin{bmatrix} I & \mathbf{0} \\ \mathbf{0} & \Lambda \end{bmatrix}. \quad (38)$$

The fourth class is of the form $[n_x, n_y, n_z] = [2, 1, 2]$, where Λ_x and Λ_z has two 1 and two -1 on the main diagonal, Λ_y has three 1 and one -1 being main diagonal entries. Then, Λ_x , Λ_y , and Λ_z are given by

$$\Lambda_x = \begin{bmatrix} \Lambda & \mathbf{0} \\ \mathbf{0} & \Lambda \end{bmatrix}, \quad \Lambda_y = \begin{bmatrix} I & \mathbf{0} \\ \mathbf{0} & \Lambda \end{bmatrix}, \quad \Lambda_z = \begin{bmatrix} \Lambda & \mathbf{0} \\ \mathbf{0} & \Lambda \end{bmatrix}. \quad (39)$$

DISCUSSION

In this paper, we investigate the contextuality of several types of infinite one-dimensional translation-invariant local quantum Hamiltonians. We found that it is very likely

that all quantum Hamiltonians with nearest-neighbor only interactions and two dichotomic observables per site admit local hidden variable models. Violation of contextuality witnesses are only possible when we either increase the interaction distance to include next-to-nearest neighbor terms or have three dichotomic observables per site. In the former case, we identified several Hamiltonians with the lowest possible ground state energy density in quantum theory. In the latter case, we give strong evidence that contextuality is only present if the dimension of local observables is greater than 2, which excludes the usual Heisenberg-type models where local observables are Pauli matrices.

States and measurements which exhibit the strongest violations of Bell inequalities are essential ingredients in device-independent certifications and self-testing (Mayers and Yao, 2004; Šupić and Bowles, 2020). So far the possibility of self-testing in quantum many-body systems has not been thoroughly established, due to a lack of tools to certify the strongest violation of Bell inequalities or contextuality witnesses, without having to solve the corresponding quantum model analytically. Our results pave the way for self-testing quantum many-body systems in the thermodynamic limit.

The ground states of our models are computed using uMPS, and they are global approximations of the true ground state of the corresponding quantum models. However, in applications such as quantum simulation, we will only have access to local approximations of the ground state. Moreover, the qualities we are interested in, such as the ground state energy density and the expectation values of local observables all depended on the accuracy of the local description. Finding locally accurate approximations of properties of one-dimensional local quantum Hamiltonians has yielded many interesting results (Dalzell and Brandão, 2019; Huang, 2015, 2019; Kuzmin *et al.*, 2022; Landau *et al.*, 2015). However, most of these results assume the models to have nearest-neighbor interactions. As we can see from our results, the models with next-to-nearest neighbor interactions are surprisingly the most interesting in terms of contextuality.

In two dimensions, very little is known about the contextuality of translation-invariant local Hamiltonians. We know that when the number of inputs and outputs is unrestricted, the set of local hidden variable models becomes non-semi-algebraic and eventually characterization of the set is impossible (Wang and Navascués, 2018). Properties of 2D classical and quantum models differ so markedly from their 1D counterparts that most intuitions and tools we gained in 1D break down. However, in 2D a powerful mathematical tool, tiling, has been repeatedly employed to solve question about computability and complexity of classical and quantum models (Cubitt *et al.*, 2015; Gottesman and Irani, 2013; Huang, 2021; Wang and Navascués, 2018). The number of tiles in an aperiodic tiling would correspond to the number of states in a local hidden variable model, so it would be interesting to explore the connection between

tiling and contextuality.

METHODS

We describe an extension of the algorithm used to minimize the ground state energy density to include the most general quantum measurements: positive operator-valued measure (POVM) measurements. The extended algorithm is used to minimize 232-type Hamiltonians when the dimension of local observables is 2. These local observables $\{\sigma_a : \mathbb{C}^2 \rightarrow \mathbb{C}^2, a \in X\}$ are constructed from POVM elements M_{a0}, M_{a1} . In a gradient descent algorithm, at iteration k the current gradient is subtracted from the parameters, which may take the local observables out of the space of POVMs. To correct this issue we project the local observables after the gradient has been subtracted onto the closest POVM found via semidefinite programming:

$$\begin{aligned} \min \quad & \|\tilde{\sigma}_a - \sigma_a\|_2 \\ \text{s.t.} \quad & \sigma_a = M_{a0} - M_{a1} \\ & M_{a0} + M_{a1} = I \\ & M_{a0} \geq 0, M_{a1} \geq 0. \end{aligned} \quad (40)$$

Here, $\tilde{\sigma}_a = \tilde{\sigma}_a(k+1)$ and $\sigma_a = \sigma_a(k+1)$. The parameters $W(k)$ are complex decision variables for the SDP, whose value at each iteration will be given by the solver.

Even though the extended algorithm based on projected gradient descent works in principle, we have encountered a number of numerical issues which require additional tweaks. The main issue affecting convergence is that it takes many iterations to traverse a nearly flat region in the parameter space. It is one of the most common problems affecting the performance of gradient descent algorithms, and it is very common to encounter such regions in our Hamiltonians. We use a well-known remedy, using momentum to speed up the traversal of nearly flat regions. At each iteration k , the parameters $W(k)$ defining the local observables $\{\sigma_a(k)|a \in X\}$ are updated by

$$V(k+1) = \eta \cdot V(k) - \gamma(k) \cdot \nabla_W e(W; k), \quad (41)$$

$$\tilde{W}(k+1) = W(k) + V(k+1), \quad (42)$$

where $V(k)$ is the momentum and η is the decay factor.

Beginning with random initial $W(0)$ and $V(0) = 0$, iterating the steps above, we obtain the a sequence of parameter values $(W(0), W(1), \dots)$ defining a sequence of local observables $(\sigma_a(0), \sigma_a(1), \dots)$, each of which is constructed from POVM elements. If the convergence criterion $|e(k+1) - e(k)| \leq \epsilon^*$ is met at a iteration k , then the algorithm stops and returns the optimal parameters $W^* \equiv W(k+1)$. For 100 out of the 652 Hamiltonians we tested, even though the random initial parameters are allowed to be complex, the converged values are all real. Having nonzero imaginary parts in the local observables meant the ground state energy of the Hamiltonian will stall

at a value higher than the classical bound, often resulting in 10000 iterations only decreasing the ground state energy marginally. When this happens, a new set of random initial complex parameters are generated and the algorithm restarts. When the algorithm converges, the imaginary parts of all the parameters are smaller than 10^{-10} .

Acknowledgments—This work is supported by the National Key R&D Program of China (No.2018YFA0306703, No.2021YFE0113100). Z.W. is supported by the Sichuan Innovative Research Team Support Fund (No. 2021JDTD0028). G.Y. is supported by the National Natural Science Foundation of China (No.62172075).

REFERENCES

- Bermejo-Vega, Juan, Nicolas Delfosse, Dan E. Browne, Cihan Okay, and Robert Raussendorf (2017), “Contextuality as a Resource for Models of Quantum Computation with Qubits,” *Phys. Rev. Lett.* **119**, 120505.
- Bouwmeester, Dik, Jian-Wei Pan, Klaus Mattle, Manfred Eibl, Harald Weinfurter, and Anton Zeilinger (1997), “Experimental quantum teleportation,” *Nature* **390** (6660), 575–579.
- Bravyi, Sergey, David Gosset, and Robert König (2018), “Quantum advantage with shallow circuits,” *Science* **362** (6412), 308–311.
- Bravyi, Sergey, David Gosset, Robert König, and Marco Tomamichel (2020), “Quantum advantage with noisy shallow circuits,” *Nature Physics* **16** (10), 1040–1045.
- Brunner, Nicolas, Daniel Cavalcanti, Stefano Pironio, Valerio Scarani, and Stephanie Wehner (2014), “Bell nonlocality,” *Rev. Mod. Phys.* **86**, 419–478.
- Budroni, Costantino, Adán Cabello, Otfried Gühne, Matthias Kleinmann, and Jan-Åke Larsson (2021), “Quantum Contextuality,” [arXiv:2102.13036](https://arxiv.org/abs/2102.13036).
- Cabello, Adán (2021), “Bell Non-locality and Kochen–Specker Contextuality: How are They Connected?” *Foundations of Physics* **51** (3), 61.
- Cubitt, Toby S, David Perez-Garcia, and Michael M. Wolf (2015), “Undecidability of the spectral gap,” *Nature* **528** (7581), 207–211.
- Dalzell, Alexander M, and Fernando G. S. L. Brandão (2019), “Locally accurate MPS approximations for ground states of one-dimensional gapped local Hamiltonians,” *Quantum* **3**, 187.
- De Chiara, Gabriele, and Anna Sanpera (2018), “Genuine quantum correlations in quantum many-body systems: a review of recent progress,” *Rep. Prog. Phys.* **81** (7), 074002.
- Gärtner, Bernd, and Jiří Matoušek (2012), *Approximation Algorithms and Semidefinite Programming*, Universitext (Springer, Berlin, Heidelberg).
- Giustina, Marissa, Marijn A. M. Versteegh, Sören Wengerowsky, Johannes Handsteiner, Armin Hochrainer, Kevin Phelan, Fabian Steinlechner, Johannes Kofler, Jan-Åke Larsson, Carlos Abellán, Waldimar Amaya, Valerio Pruneri, Morgan W. Mitchell, Jörn Beyer, Thomas Gerrits, Adriana E. Lita, Lynden K. Shalm, Sae Woo Nam, Thomas Scheidl, Rupert Ursin, Bernhard Wittmann, and Anton Zeilinger (2015), “Significant-Loophole-Free Test of Bell’s Theorem with Entangled Photons,” *Phys. Rev. Lett.* **115**, 250401.
- Goldstein, Sheldon, Tobias Kuna, Joel Louis Lebowitz, and Eugene Richard Speer (2017), “Translation Invariant Extensions of Finite Volume Measures,” *Journal of Statistical Physics* **166** (3), 765–782.
- Gottesman, Daniel, and Sandy Irani (2013), “The Quantum and Classical Complexity of Translationally Invariant Tiling and Hamiltonian Problems,” *Theory of Computing* **9** (2), 31–116.
- Haegeman, Jutho, J. Ignacio Cirac, Tobias J. Osborne, Iztok Pižorn, Henri Verschelde, and Frank Verstraete (2011), “Time-Dependent Variational Principle for Quantum Lattices,” *Phys. Rev. Lett.* **107**, 070601.
- Hensen, Bas, Hannes Bernien, Anaïs E. Dréau, Andreas Reiserer, Norbert Kalb, Machiel Sebastiaan Blok, Just Ruitenberg, Raymond F. L. Vermeulen, Raymond N. Schouten, Carlos Abellán, Waldimar Amaya, Valerio Pruneri, Morgan W. W. Mitchell, Matthew Markham, Daniel J. Twitchen, David Elkouss, Stephanie Wehner, Tim Hugo Taminiau, and Ronald Hanson (2015), “Loophole-free Bell inequality violation using electron spins separated by 1.3 kilometres,” *Nature* **526**, 682–686.
- Howard, Mark, Joel Wallman, Victor Veitch, and Joseph Emerson (2014), “Contextuality supplies the ‘magic’ for quantum computation,” *Nature* **510** (7505), 351–355.
- Huang, Yichen (2015), “Computing energy density in one dimension,” [arXiv:1505.00772](https://arxiv.org/abs/1505.00772).
- Huang, Yichen (2019), “Approximating local properties by tensor network states with constant bond dimension,” [arXiv:1903.10048](https://arxiv.org/abs/1903.10048).
- Huang, Yichen (2021), “Two-dimensional local Hamiltonian problem with area laws is QMA-complete,” *Journal of Computational Physics* **443**, 110534.
- Ji, Zhengfeng, Anand Natarajan, Thomas Vidick, John Wright, and Henry Yuen (2020), “MIP*=RE,” [arXiv:2001.04383](https://arxiv.org/abs/2001.04383).
- Kochen, Simon Bernhard, and Ernst Paul Specker (1967), “The Problem of Hidden Variables in Quantum Mechanics,” *J. Math. Mech.* **17** (1), 59–87.
- Kuzmin, Viacheslav, Torsten V. Zache, Christian Kokail, Lorenzo Pastori, Alessio Celi, Mikhail Baranov, and Peter Zoller (2022), “Probing infinite many-body quantum systems with finite-size quantum simulators,” *PRX Quantum* **3**, 020304.
- Landau, Zeph, Umesh Vazirani, and Thomas Vidick (2015), “A polynomial time algorithm for the ground state of one-dimensional gapped local Hamiltonians,” *Nature Physics* **11** (7), 566–569.
- Matoušek, Jiří, and Bernd Gärtner (2007), *Understanding and Using Linear Programming*, Universitext (Springer, Berlin, Heidelberg).
- Mayers, Dominic, and Andrew Yao (2004), “Self testing quantum apparatus,” *Quantum Information & Computation* **4** (4), 273–286.
- Milsted, Ashley, Jutho Haegeman, Tobias J. Osborne, and Frank Verstraete (2013), “Variational matrix product ansatz for nonuniform dynamics in the thermodynamic limit,” *Phys. Rev. B* **88**, 155116.
- Navascués, Miguel, Stefano Pironio, and Antonio Acín (2007), “Bounding the Set of Quantum Correlations,” *Phys. Rev. Lett.* **98**, 010401.
- Navascués, Miguel, Stefano Pironio, and Antonio Acín (2008), “A convergent hierarchy of semidefinite programs characterizing the set of quantum correlations,” *New Journal of Physics* **10** (7), 073013.
- Peruzzo, Alberto, Jarrod McClean, Peter Shadbolt, Man-Hong Yung, Xiao-Qi Zhou, Peter J. Love, Alán Aspuru-Guzik, and Jeremy L. O’Brien (2014), “A variational eigenvalue solver on a photonic quantum processor,” *Nature Communications* **5** (1), 4213.
- Popescu, Sandu, and Daniel Rohrlich (1994), “Quantum nonlocal-

- ity as an axiom,” *Foundations of Physics* **24** (3), 379–385.
- Rosset, Denis (2015), *Characterization of correlations in quantum networks*, Ph.D. thesis (Université de Genève).
- Scarani, Valerio (2019), *Bell Nonlocality* (Oxford University Press).
- Schmied, Roman, Jean-Daniel Bancal, Baptiste Allard, Matteo Fadel, Valerio Scarani, Philipp Treutlein, and Nicolas Sangouard (2016), “Bell correlations in a Bose-Einstein condensate,” *Science* **352** (6284), 441–444.
- Shalm, Lynden K, Evan Meyer-Scott, Bradley G. Christensen, Peter Bierhorst, Michael A. Wayne, Martin J. Stevens, Thomas Gerrits, Scott Glancy, Deny R. Hamel, Michael S. Allman, Kevin J. Coakley, Shellee D. Dyer, Carson Hodge, Adriana E. Lita, Varun B. Verma, Camilla Lambrocco, Edward Tortorici, Alan L. Migdall, Yanbao Zhang, Daniel R. Kumor, William H. Farr, Francesco Marsili, Matthew D. Shaw, Jeffrey A. Stern, Carlos Abellán, Waldimar Amaya, Valerio Pruneri, Thomas Jennewein, Morgan W. Mitchell, Paul G. Kwiat, Joshua C. Bienfang, Richard P. Mirin, Emanuel Knill, and Sae Woo Nam (2015), “Strong Loophole-Free Test of Local Realism,” *Phys. Rev. Lett.* **115**, 250402.
- Šupić, Ivan, and Joseph Bowles (2020), “Self-testing of quantum systems: a review,” *Quantum* **4**, 337.
- The OEIS Foundation Inc., (2021a), “[The On-Line Encyclopedia of Integer Sequences: A027691](#),” .
- The OEIS Foundation Inc., (2021b), “[The On-Line Encyclopedia of Integer Sequences: A152948](#),” .
- Tura, Jordi, Remigiusz Augusiak, Ana Belén Sainz, Bernd Lücke, Carsten Klempt, Maciej Lewenstein, and Antonio Acín (2015), “Nonlocality in many-body quantum systems detected with two-body correlators,” *Annals of Physics* **362**, 370 – 423.
- Tura, Jordi, Remigiusz Augusiak, Ana Belén Sainz, Tamas Vértesi, Maciej Lewenstein, and Antonio Acín (2014a), “Detecting nonlocality in many-body quantum states,” *Science* **344** (6189), 1256–1258.
- Tura, Jordi, Gemma De las Cuevas, Remigiusz Augusiak, Maciej Lewenstein, Antonio Acín, and J. Ignacio Cirac (2017), “Energy as a Detector of Nonlocality of Many-Body Spin Systems,” *Phys. Rev. X* **7**, 021005.
- Tura, Jordi, Ana Belén Sainz, Tamás Vértesi, Antonio Acín, Maciej Lewenstein, and Remigiusz Augusiak (2014b), “Translationally invariant multipartite Bell inequalities involving only two-body correlators,” *Journal of Physics A: Mathematical and Theoretical* **47** (42), 424024.
- Vanderstraeten, Laurens, Jutho Haegeman, and Frank Verstraete (2019), “Tangent-space methods for uniform matrix product states,” *SciPost Phys. Lect. Notes* , 7.
- Wang, Zizhu, and Miguel Navascués (2018), “Two-dimensional translation-invariant probability distributions: approximations, characterizations and no-go theorems,” *Proceedings of the Royal Society A: Mathematical, Physical and Engineering Sciences* **474** (2217), 20170822.
- Wang, Zizhu, Sukhwinder Singh, and Miguel Navascués (2017), “Entanglement and Nonlocality in Infinite 1D Systems,” *Phys. Rev. Lett.* **118**, 230401.
- Zauner-Stauber, Valentin, Laurens Vanderstraeten, Matthew T. Fishman, Frank Verstraete, and Jutho Haegeman (2018), “Variational optimization algorithms for uniform matrix product states,” *Phys. Rev. B* **97**, 045145.
- Zurel, Michael, Cihan Okay, and Robert Raussendorf (2020), “Hidden Variable Model for Universal Quantum Computation with Magic States on Qubits,” *Phys. Rev. Lett.* **125**, 260404.

Appendix A: Couplings and quantum values of the 322-type Hamiltonians

Out of the 2102 equivalent classes of 322-type Hamiltonians, our algorithm found 63 which can violate the classical bound. Table V lists their couplings and the corresponding classical bounds (\mathcal{L}). Table VI gives lowest the ground state energy density (\mathcal{Q}) with d -dimensional local observables. The optimal parameters to reconstruct these local observables (w), the numbers of -1 in the eigenvalues of each local observable ($[n_x, n_y]$), the bond dimension of the uMPS describing the ground state (D), and the LTI_5 -NPA₁ lower bound are also given.

Appendix B: Couplings and parameters of the 232-type Hamiltonians

Table VII gives the couplings, classical bounds (\mathcal{L}) of five 232-type TI Hamiltonians presented in the main text. The parameters defining local observables and the numbers of -1 in the eigenvalues of each local observables ($[n_x, n_y, n_z]$) are presented in Table VIII when $d = 3$ and in Table IX when $d = 4$.

TABLE V Couplings and classical bounds for 63 322-type Hamiltonians.

No.	\mathcal{L}	J_x	J_y	J_{xx}^{AB}	J_{xy}^{AB}	J_{yx}^{AB}	J_{yy}^{AB}	J_{xx}^{AC}	J_{xy}^{AC}	J_{yx}^{AC}	J_{yy}^{AC}
1	-6	-6	0	2	3	3	-2	3	-1	-1	1
2	-6	-4	2	2	2	2	-4	1	-1	-1	3
3	-3	-3	1	1	1	1	-1	1	0	-1	1
4	-4	-2	-2	-2	1	-1	-2	1	0	2	1
5	-8	-11	1	5	2	2	-1	4	-1	-2	1
6	-4	-3	-3	2	2	-1	2	1	1	-1	0
7	-5	-3	-3	2	2	2	-3	1	0	-1	2
8	-4	-2	-4	-2	2	2	2	1	0	0	1
9	-4	0	-4	2	2	-2	2	0	1	-1	0
10	-5	-2	2	2	-2	-2	-4	1	1	1	2
11	-3	-1	1	2	-1	-1	-2	1	1	0	1
12	-6	-2	-6	-2	4	3	3	1	-1	0	2
13	-11	6	-8	4	2	-8	5	-2	1	-7	0
14	-16	8	-12	5	2	-12	7	-4	1	-11	0
15	-6	3	-5	2	1	-4	3	-1	1	-3	1
16	-7	-6	4	4	2	-4	3	0	1	-3	0
17	-14	-12	6	7	2	-10	4	0	1	-9	-3
18	-9	-8	4	5	2	-6	3	0	1	-5	-1
19	-11	-4	-12	-4	6	6	6	1	-1	-1	4
20	-4	-1	-5	-1	2	2	2	0	0	-1	2
21	-4	-3	1	3	-2	-2	-1	2	1	0	1
22	-5	-6	0	2	2	1	-2	2	0	-1	1
23	-8	-8	2	4	-4	-4	-4	3	1	1	1
24	-7	-5	-5	2	3	2	-4	1	1	-1	3
25	-8	-3	-7	-2	4	5	4	2	0	-2	3
26	-4	2	-4	1	1	-3	2	-1	0	-2	0
27	-3	-2	-2	2	2	-1	1	0	1	0	0
28	-3	-2	0	1	2	1	-2	1	-1	0	1
29	-4	-4	2	2	-1	-2	-2	1	0	-1	1
30	-4	-1	-5	1	2	-1	3	0	1	-1	1
31	-8	-6	-6	3	6	-2	3	-1	3	1	-1
32	-7	-3	3	-5	3	2	2	4	-1	-1	1
33	-3	-1	-3	-1	2	1	2	0	0	0	1
34	-6	-4	-4	2	5	-1	2	-1	4	0	-1
35	-6	-4	-6	-3	3	2	2	2	1	0	1
36	-6	-4	-4	2	5	-1	2	-1	3	1	-1
37	-6	-4	4	3	2	-3	4	0	1	-2	1
38	-4	-4	0	1	2	2	-1	2	-1	-1	0
39	-5	-3	1	-4	2	1	1	3	-1	-1	0
40	-4	-1	1	-3	2	2	1	2	0	-1	1
41	-15	5	-3	4	9	7	-9	5	-5	2	6
42	-5	-1	-5	-1	3	1	4	0	0	-1	3
43	-6	2	0	-5	3	3	1	3	-1	-1	1
44	-11	-3	-11	-3	7	5	6	2	-2	-1	5
45	-6	-2	-6	-2	3	3	4	1	-1	-1	3
46	-6	-4	0	-5	2	2	1	4	-1	-1	0
47	-4	-2	2	1	1	1	-3	0	-1	-1	2
48	-10	-4	4	-5	3	-2	-6	2	-6	1	3
49	-8	-4	2	-6	3	3	2	5	-1	-1	1
50	-7	-6	2	5	1	-5	1	1	0	-4	-2
51	-10	4	-8	3	2	-7	6	-2	1	-6	1
52	-4	-2	2	1	0	-1	2	2	1	-2	1
53	-13	12	4	7	8	6	-3	6	-3	-1	3
54	-6	-6	2	5	2	-3	2	1	1	-2	0
55	-8	5	-3	1	-3	-5	-1	4	1	-4	1
56	-7	-7	1	6	1	-4	1	2	1	-3	-1
57	-5	-1	5	0	0	0	4	-1	-1	-2	3
58	-7	-6	2	5	0	-2	-1	4	1	-3	1
59	-8	6	-2	5	-1	-1	1	4	-2	-4	-2
60	-8	-6	-8	-4	3	3	2	3	1	1	1
61	-5	-3	3	-3	-1	-2	2	2	1	-1	1
62	-7	6	-2	6	0	-1	-1	3	-1	-4	-1
63	-5	-3	-3	0	3	1	-1	1	-2	1	2

TABLE VI Ground state energy density, optimal parameters, type of parameterized observables and bond dimension of 63 322-type Hamiltonians under the different dimensions of local observables.

No.	\mathcal{L}	$d = 2$				$d = 3$				$d = 4$				$d = 5$				LTI ₅ -NPA ₁		
		\mathcal{Q}_2	w_1	$[n_x, n_y]$	D	\mathcal{Q}_3	w_1	$[n_x, n_y]$	D	\mathcal{Q}_4	w_1	w_2	$[n_x, n_y]$	D	\mathcal{Q}_5	w_1	w_2		$[n_x, n_y]$	D
1	-6	-6.08108	1.2472	[1, 1]	7	-6.32747	0.7811	[1, 2]	5											-6.32747
2	-6	-6.10943	1.2224	[1, 1]	7	-6.33712	0.9117	[1, 2]	5											-6.33712
3	-3	-3.04150	1.2508	[1, 1]	8	-3.20711	0.7852	[1, 2]	5											-3.20711
4	-4	-	-	-	-	-4.14623	0.7925	[1, 1]	5											-4.14623
5	-8	-	-	-	-	-8.12123	0.6735	[1, 2]	5											-8.12123
6	-4	-	-	-	-	-4.02415	0.3641	[1, 1]	16	-4.10310	-0.0000	0.7031	[2, 2]	6						-4.10310
7	-5	-	-	-	-	-5.09951	1.1158	[1, 1]	12	-5.09951	0.0000	-1.1156	[2, 2]	12	-5.29852	1.5704	0.8509	[2, 2]	6	-5.29852
8	-4	-	-	-	-	-4.18655	0.9483	[1, 1]	14	-4.18655	-0.9483	0.0000	[2, 2]	14	-4.33137	1.5699	0.7854	[2, 2]	6	-4.33137
9	-4	-	-	-	-	-4.11581	1.1034	[1, 1]	14	-4.11581	0.4671	1.5708	[2, 2]	15	-4.41421	0.7854	1.5702	[2, 2]	5	-4.41421
10	-5	-	-	-	-	-5.07058	0.3947	[1, 2]	12	-5.07058	0.3948	1.5708	[2, 2]	12	-5.26969	1.5708	0.6590	[3, 3]	6	-5.26969
11	-3	-	-	-	-	-3.00628	0.3540	[1, 2]	8	-3.00628	0.3533	1.5708	[2, 2]	8	-3.11696	0.7857	1.5704	[3, 3]	6	-3.11696
12	-6	-	-	-	-	-6.06459	0.4885	[1, 1]	14	-6.20259	0.0000	0.7000	[2, 2]	6						-6.20261
13	-11	-	-	-	-	-	-	-	-	-11.19018	-1.5708	-2.2493	[2, 2]	6						-11.19036
14	-16	-	-	-	-	-	-	-	-	-16.17635	0.8977	1.5708	[2, 2]	6						-16.17654
15	-6	-	-	-	-	-	-	-	-	-6.09323	1.5708	0.8916	[2, 2]	6						-6.09347
16	-7	-	-	-	-	-	-	-	-	-7.21677	1.5708	0.8683	[2, 2]	6						-7.21747
17	-14	-	-	-	-	-	-	-	-	-14.18216	-1.5708	2.2462	[2, 2]	6						-14.18291
18	-9	-	-	-	-	-	-	-	-	-9.20253	1.5708	0.8852	[2, 2]	6						-9.20406
19	-11	-	-	-	-	-11.40483	0.6551	[1, 1]	14	-11.47642	0.0000	-0.7229	[2, 2]	6						-11.47839
20	-4	-4.00682	1.2170	[1, 1]	4	-4.02137	0.4173	[1, 1]	16	-4.12887	1.5708	0.7030	[2, 2]	5						-4.13251
21	-4	-	-	-	-	-	-	-	-	-4.06491	1.5708	0.9817	[2, 2]	6						-4.06890
22	-5	-5.00062	1.3959	[1, 1]	4	-5.12457	0.7855	[1, 2]	5	-5.12457	1.5708	0.7854	[2, 2]	5						-5.12887
23	-8	-8.01053	0.2887	[1, 1]	5	-8.13694	0.6619	[1, 1]	5	-8.13694	0.0000	0.6618	[2, 2]	5						-8.14126
24	-7	-	-	-	-	-7.11178	1.1000	[1, 1]	12	-7.11178	0.0000	1.1002	[2, 2]	12	-7.25367	0.8707	1.5704	[2, 2]	6	-7.25827
25	-8	-	-	-	-	-8.00096	0.1630	[1, 1]	16	-8.14914	0.0000	0.6379	[2, 2]	6						-8.15428
26	-4	-	-	-	-	-	-	-	-	-4.07800	1.5708	1.0105	[2, 2]	6	-4.14354	0.8877	1.5707	[2, 2]	5	-4.14877
27	-3	-	-	-	-	-3.11927	0.8353	[1, 1]	8	-3.11932	0.0000	0.7027	[2, 2]	6	-3.14915	0.7027	1.5694	[2, 2]	5	-3.15470
28	-3	-3.04030	1.2555	[1, 1]	7	-3.14915	0.8685	[1, 2]	5	-3.14915	0.8682	1.5708	[2, 2]	5						-3.15470
29	-4	-	-	-	-	-	-	-	-	-4.00935	1.3742	0.3202	[2, 2]	12	-4.09966	1.5708	0.7860	[3, 3]	7	-4.10571
30	-4	-	-	-	-	-4.03262	0.3966	[1, 1]	19	-4.11218	0.0000	0.7054	[2, 2]	6	-4.14023	0.7054	1.5699	[2, 2]	5	-4.14877
31	-8	-	-	-	-	-	-	-	-	-8.22037	0.0000	0.6827	[2, 2]	6						-8.23071
32	-7	-7.08653	1.2383		6	-7.25928	0.9558	[1, 2]	5	-7.25928	0.9558	1.5708	[2, 2]	5						-7.27038
33	-3	-	-	-	-	-3.11932	0.7018	[1, 1]	6	-3.11932	0.0000	0.7026	[2, 2]	6						-3.13058
34	-6	-	-	-	-	-	-	-	-	-6.03951	0.0000	0.4637	[2, 2]	6						-6.05216
35	-6	-	-	-	-	-6.19072	0.9694	[1, 1]	14	-6.19072	0.0000	0.9700	[2, 2]	14	-6.26479	0.8478	1.5702	[2, 2]	6	-6.27801
36	-6	-	-	-	-	-	-	-	-	-6.03951	0.0000	0.4637	[2, 2]	6						-6.05327
37	-6	-	-	-	-	-	-	-	-	-6.17482	1.5708	0.8827	[2, 2]	6						-6.18885
38	-4	-4.03281	1.2745	[1, 1]	8	-4.14623	0.7767	[1, 2]	5	-4.14623	1.5708	0.7775	[2, 2]	5						-4.16445
39	-5	-5.06166	1.9574	[1, 1]	7	-5.12466	0.9504	[1, 2]	7	-5.12466	1.5708	0.9503	[2, 2]	7						-5.14311
40	-4	-4.02193	1.3015	[1, 1]	5	-4.06591	1.0457	[1, 2]	5	-4.06591	1.0459	1.5708	[2, 2]	5						-4.08498
41	-15	-15.01150	1.3600	[1, 1]	5	-15.01150	1.7814	[1, 1]	5	-15.13717	4.1651	1.5708	[2, 2]	5						-15.15803
42	-5	-	-	-	-	-	-	-	-	-5.01755	0.7989	0.0884	[2, 2]	16	-5.04311	0.2159	0.7668	[2, 2]	12	-5.06400
43	-6	-6.01649	1.8170	[1, 1]	5	-6.01649	1.8170	[1, 1]	6	-6.04536	1.1166	1.5708	[2, 2]	8						-6.06803
44	-11	-	-	-	-	-11.00119	0.1638	[1, 1]	12	-11.15383	0.0000	0.5575	[2, 2]	6						-11.17826
45	-6	-	-	-	-	-6.18037	0.6128	[1, 1]	16	-6.22875	0.0000	0.7013	[2, 2]	6						-6.25396
46	-6	-6.06990	1.9751	[1, 1]	6	-6.12318	0.9210	[1, 2]	7	-6.12318	1.5708	0.9210	[2, 2]	7						-6.14907
47	-4	-4.07352	1.1798	[1, 1]	7	-4.15468	0.9590	[1, 2]	5	-4.15469	1.5708	0.9587	[2, 2]	5						-4.18142
48	-10	-	-	-	-	-	-	-	-	-10.14203	0.9241	-1.5708	[2, 2]	5						-10.17428
49	-8	-8.07815	1.2431	[1, 1]	7	-8.18189	1.0153	[1, 2]	5	-8.18189	1.5708	1.0152	[2, 2]	5						-8.21614
50	-7	-	-	-	-	-	-	-	-	-7.00917	0.7748	-1.6163	[2, 2]	12						-7.04393
51	-10	-	-	-	-	-	-	-	-	-10.10510	-0.9808	1.5708	[2, 2]	6						-10.14126
52	-4	-	-	-	-	-	-	-	-	-4.08523	1.5708	0.8681	[2, 2]	9						-4.12479
53	-13	-	-	-	-	-	-	-	-	-13.10714	0.0000	-0.5039	[2, 2]	7						-13.14828
54	-6	-	-	-	-	-	-	-	-	-6.16786	0.8899	1.5708	[2, 2]	6						-6.21564
55	-8	-	-	-	-	-	-	-	-	-8.00371	2.3012	-1.5949	[2, 2]	16						-8.05192
56	-7	-	-	-	-	-	-	-	-	-7.01064	0.8015	1.6238	[2, 2]	12						-7.05935
57	-5	-	-	-	-	-	-	-	-	-5.05572	1.5708	1.0099	[2, 2]	9						-5.10699
58	-7	-	-	-	-	-	-	-	-	-7.00144	0.3372	1.5603	[2, 2]	11						-7.05714
59	-8	-	-	-	-	-	-	-	-	-8.17045	-1.5708	0.8676	[2, 2]	9	-8.17045	0.8686	1.5708	[2, 2]	9	-8.24220
60	-8	-	-	-	-	-8.22013	0.9539	[1, 1]	5	-8.22013	0.0000	0.9539	[2, 2]	5						-8.29902
61	-5	-	-	-	-	-5.00822	0.3766	[1, 2]	11	-5.00822	0.3774	1.5708	[2, 2]	11						-5.09824
62	-7	-	-	-	-	-	-	-	-	-7.00638	2.1879	1.5295	[2, 2]	24						-7.10456
63	-5	-	-	-	-	-5.00639	1.3547	[1, 1]	8	-5.00639	1.3556	0.0000	[2, 2]	8						-5.13037

TABLE VII Couplings for 5 232-type TI Hamiltonians presented in Table IV.

No.	\mathcal{L}	J_x	J_y	J_z	J_{xx}	J_{xy}	J_{xz}	J_{yx}	J_{yy}	J_{yz}	J_{zx}	J_{zy}	J_{zz}
1	-9	3	-2	1	2	-2	5	-1	1	3	1	-2	-2
2	-4	2	1	1	2	2	1	0	-1	0	-1	1	0
3	-5	2	-1	1	1	-1	2	-2	0	2	-1	0	0
4	-4	1	-1	0	1	1	2	0	1	-1	0	1	-1
5	-2	0	0	0	1	1	0	0	0	0	-1	1	0

TABLE VIII Parameters of 5 232-type TI Hamiltonians under the bond dimension $D = 10$ and the dimension of local observables $d = 3$.

No.	\mathcal{L}	$d = 3$									
		w_1	w_2	w_3	w_4	w_5	w_6	w_7	w_8	w_9	$[n_x, n_y, n_z]$
1	-9	0.3392	0.1055	0.4115	0.4133	0.3652	0.9916	0.4810	-0.0351	-0.3163	[2, 1, 1]
2	-4	0.5943	0.0469	0.2011	0.2756	0.4268	0.1822	0.0277	0.7213	0.1413	[2, 1, 2]
3	-5	1.0061	-0.0081	0.2303	0.3148	0.0616	0.5666	-0.2498	0.2271	0.0076	[2, 1, 2]
4	-4	0.1303	-0.0032	0.5139	0.2574	0.4723	0.6582	0.3285	-0.1727	0.2820	[2, 1, 1]
5	-2	0.4899	-0.1481	0.1905	0.4931	0.4919	0.3638	-0.1067	0.7160	0.2088	[2, 1, 2]

TABLE IX Parameters of 5 232-type TI Hamiltonians under the bond dimension $D = 10$ and the dimension of local observables $d = 4$.

No.	\mathcal{L}	$d = 4$																		
		w_1	w_2	w_3	w_4	w_5	w_6	w_7	w_8	w_9	w_{10}	w_{11}	w_{12}	w_{13}	w_{14}	w_{15}	w_{16}	w_{17}	w_{18}	$[n_x, n_y, n_z]$
1	-9	-0.0270	0.2185	0.0934	0.2068	0.3829	0.3010	0.3126	0.3287	0.2716	0.1611	-0.2841	-0.4393	0.1235	0.1030	0.1933	0.1480	0.6689	1.0601	[3, 1, 1]
2	-4	0.4490	0.5450	0.4828	0.0387	0.1335	0.1225	0.2003	0.2535	0.2878	0.0661	0.2800	0.1061	0.0102	-0.0804	0.0821	0.0320	0.3449	0.0535	[3, 2, 3]
3	-5	0.5565	1.2916	0.8706	0.1371	0.1162	0.9160	0.4551	0.5068	0.1782	0.4305	0.8979	0.1097	0.2928	-0.4064	0.1088	0.7717	0.6469	0.9466	[3, 2, 3]
4	-4	-0.2912	0.2321	0.0211	0.0911	0.2954	0.0986	0.6905	0.3049	0.3104	0.2755	0.1093	0.1728	0.0995	0.4044	-0.0148	0.1701	0.2056	0.4232	[3, 2, 1]
5	-2	0.4998	0.0447	-0.3366	-0.0197	0.3869	-0.0971	0.2528	0.2196	0.5018	0.0579	0.1594	0.2374	0.0932	0.1598	0.5637	0.5072	0.2408	0.2743	[2, 1, 2]